Modulation of the p K a of Metal−Bound Water via Oxidation of Thiolato Sulfur in Model Complexes of Co(III) Containing Nitrile Hydratase: Insight into Possible Effect of Cysteine O...

ARTICLE *in* INORGANIC CHEMISTRY · OCTOBER 2003

Impact Factor: 4.76 · DOI: 10.1021/ic030088s · Source: PubMed

4 AUTHORS, INCLUDING:

Marilyn M. Olmstead
University of California, Davis
951 PUBLICATIONS **26,092** CITATIONS
SEE PROFILE

Pradip K. Mascharak
University of California, Santa Cruz
234 PUBLICATIONS **6,698** CITATIONS
SEE PROFILE

Inorg. Chem. **2003**, *42*, 5751–5761

Modulation of the pK_a of Metal-Bound Water via Oxidation of Thiolato Sulfur in Model Complexes of Co(III) Containing Nitrile Hydratase: Insight into Possible Effect of Cysteine Oxidation in Co–Nitrile Hydratase

Laurie A. Tyler, Juan C. Noveron, Marilyn M. Olmstead, and Pradip K. Mascharak*

Department of Chemistry and Biochemistry, University of California, Santa Cruz, California 95064, and Department of Chemistry, University of California, Davis, California 95616

Received March 7, 2003

The Co(III) complexes of *N*,*N*′-bis(2-mercaptophenyl)pyridine-2,6-dicarboxamide ($PyPSH_4$), a designed pentadentate ligand with built-in carboxamide and thiolate groups, have been synthesized and studied to gain insight into the role of Cys-S oxidation in Co-containing nitrile hydratase (Co–NHase). Reaction of $[Co(NH_3)_5Cl]Cl_2$ with $PyPS^{4-}$ in DMF affords the thiolato-bridged dimeric Co(III) complex $(Et_4N)_2[Co_2(PyPS)_2]$ (**1**). Although the bridged structure is quite robust, reaction of $(Et_4N)(CN)$ with **1** in acetonitrile affords the monomeric species $(Et_4N)_2[Co(PyPS)(CN)]$ (**2**). Oxidation of **2** with H_2O_2 in acetonitrile gives rise to a mixture which, upon chromatographic purification, yields $K_2[Co(PyPSO_2(OSO_2)(CN]$ (**3**), a species containing asymmetrically oxidized thiolates. The Co(III) metal center in **3** is coordinated to a S-bound sulfinate and an O-bound sulfonate (OSO_2) group. Upon oxidation with H_2O_2, **1** affords an asymmetrically oxidized dimer $(Et_4N)_2[Co_2(PyPS(SO_2))_2]$ (**4**) in which only the terminal thiolates are oxidized to form S-bound sulfinate groups while the bridging thiolates remain unchanged. The thiolato-bridge in **4** is also cleaved upon reaction with $(Et_4N)(CN)$ in acetonitrile, and one obtains $(Et_4N)_2[Co(PyPS(SO_2))(CN)]$ (**5**), a species that contains both coordinated thiolate and S-bound sulfinate around Co(III). The structures of **1**–**4** have been determined. The spectroscopic properties and reactivity of all the complexes have been studied to understand the behavior of the Co(III) site in Co–NHase. Unlike typical Co(III) complexes with bound CN^- ligands, the Co(III) centers in **2** and **5** are labile and rapidly lose CN^- in aqueous solutions. Since **3** does not show this lability, it appears that at least one thiolato sulfur donor is required in the first coordination sphere for the Co(III) center in such species to exhibit lability. Both **2** and **5** are converted to the aqua complexes $[Co(PyPS)(H_2O)]^-$ and $[Co(PyPS(SO_2)(H_2O)]^-$ in aqueous solutions. The pK_a values of the bound water in these two species, determined by spectrophotometry, are 8.3 ± 0.03 and 7.2 ± 0.06, respectively. Oxidation of the thiolato sulfur (to sulfinate) therefore increases the acidity of the bound water. Since **2** and **5** promote hydrolysis of acetonitrile at pH values above their corresponding pK_a values, it is also evident that a metal-bound hydroxide is a key player in the mechanism of hydrolysis by these model complexes of Co–NHase. The required presence of a Cys-sulfinic residue and one water molecule at the Co(III) site of Co–NHase as well as the optimal pH of the enzyme near 7 suggests that (i) modulation of the pK_a of the bound water molecule at the active site of the enzyme could be one role of the oxidized Cys-S residue(s) and (ii) a cobalt-bound hydroxide could be responsible for the hydrolysis of nitriles by Co–NHase.

Introduction

In recent years, enzymatic processes that convert otherwise resilient substrates into commercially useful products at ambient conditions have drawn much attention.[1] One such enzyme is nitrile hydratase (NHase) which catalyzes the conversion of a variety of nitriles to the corresponding amides

* To whom correspondence should be addressed. E-mail: mascharak@chemistry.ucsc.edu.

(1) Drauz, K.; Waldmann, H. *Enzyme Catalysis in Organic Synthesis*; VCH: Weinheim, Federal Republic of Germany, 1995.

10.1021/ic030088s CCC: $25.00
Published on Web 08/13/2003

in several microorganisms.[2−6] This enzyme has found use in several industrial processes. For example, NHase is currently employed in the industrial production of high purity acrylamide in multi-kiloton scales.[7−9] Current synthetic methods (nonmicrobial) employed in the production of amides from nitriles require harsh reaction conditions (high acidity or alkalinity), consumption of large amount of energy, and the production of unwanted byproducts.[1] The chemical processes are therefore not only are costly but also result in the production of hazardous byproducts. For these reasons, enzymatic production of amides under mild conditions is preferable. In addition, NHases have also found wide use as environmental remediation catalysts.[10−12]

NHases exist as $\alpha\beta$ 46 kDa heterodimers or $(\alpha\beta)_2$ 92 kDa tetramers and contain either a low spin non-heme Fe(III) or non-corrin Co(III) at the active site coordinated to amino acid residues of the α subunit.[13,14] Recent crystallographic analysis of the Co-containing NHase (Co−NHase), *Pseudonocardia thermophila* JCM 3095,[15] reveals that the structure of this Co−NHase is similar to the structure reported for the Fe-containing NHase (Fe−NHase), *Rhodococcus* sp. N-772.[16] The coordination sphere around the M(III) centers in both Fe− and Co−NHases are nearly identical. Each metal center is ligated to two deprotonated carboxamido nitrogens and three cysteinate groups, two of which are post-translationally modified to Cys-sulfenic (SOH) and -sulfinic (SO_2H) acids. However, the sixth site of the Co(III) metal center contains a water molecule while the analogous site in Fe−NHase is occupied by an exogenous NO molecule. Fe−NHases are photoactivated by the reversible binding of NO[17−21] and the post-translational oxidation of the Cys-S residues is believed to help stabilize the inactive (dark) NO-bound form of the enzyme. For Fe−NHases, the post-translational oxidation of the Cys-S residues has been shown to be essential for catalytic activity of the enzyme.[22] Since Co−NHases do not bind NO or exhibit similar photoactivation, the purpose of cysteine oxidation in Co−NHases remains unclear.

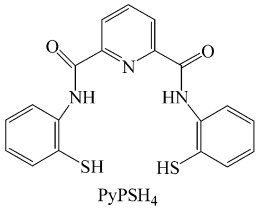

$PyPSH_4$

Recently, we reported a Co(III) complex of the designed pentadentate ligand $PyPSH_4$ (H's denote dissociable protons) as the first functional model of Co−NHase.[23] Initial reactions of $PyPS^{4-}$ with Co(III) starting material resulted in the isolation of a dimeric complex, $(Et_4N)_2[Co_2(PyPS)_2]$ (**1**), that reacts with $(Et_4N)(CN)$ to afford a monomeric species, $(Et_4N)_2[Co(PyPS)(CN)]$ (**2**). Surprisingly, the Co(III) metal center in **2** is labile and in aqueous media rapidly loses CN^- to afford the aqua complex $[Co(PyPS)(H_2O)]^-$. The coordination structure of the Co(III) metal center in this species is similar to that reported for the Co(III) site in Co−NHase. The pK_a of the bound water molecule in $[Co(PyPS)(H_2O)]^-$ is 8.3 ± 0.03, and this model complex hydrolyzes CH_3CN in aqueous buffer (pH > 9) at an appreciable rate above 40 °C.[23] It appears that a Co(III)-bound hydroxide could be responsible for the hydration of nitriles. Indeed, such a mechanism has been proposed by several groups although the exact steps leading to the formation of amides have not been identified.[2,13] This fact underscores the importance of the pK_a of bound water in model complexes such as $[Co(PyPS)(H_2O)]^-$.

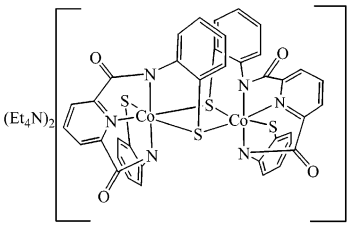

$(Et_4N)_2[Co_2(PyPS)_2]$ (**1**)

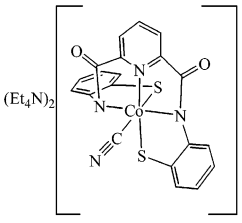

$(Et_4N)_2[Co(PyPS)(CN)]$ (**2**)

We[24−26] and others[27−30] have previously shown that model complexes of Co−NHase containing thiolato sulfurs in

(2) Kobayashi, M.; Shimizu, S. *Curr. Opin. Chem. Biol.* **2000**, *4*, 95−102.
(3) Endo, I.; Odaka, M.; Yohda, M. *Trends Biotechnol*. **1999**, *17*, 244−248.
(4) Nagasawa, T.; Shimizu, H.; Yamada, H. *Appl. Microbiol. Biotechnol.* **1993**, *40*, 189−193.
(5) Amarant, T.; Vered, Y.; Bohak, Z. *Biotechnol. Appl. Biochem.* **1989**, *11*, 49−59.
(6) Nagasawa, T.; Yamada, H. *Trends Biotechnol*. **1989**, *7*, 153−158.
(7) Yamada, H.; Kobayashi, M. *Biosci. Biotechnol. Biochem*. **1996**, *60* (90), 1391−1400.
(8) Yamada, H.; Kobayashi, M. *Trends Biotechnol*. **1992**, *10*, 402−408.
(9) Nagasawa, T.; Ryuno, K.; Yamada, H. *Experimentia* **1989**, *45*, 1066−1070.
(10) Kobayashi, S. Shimizu, S. *Nature Biotechnol.* **1998**, *16*, 733−736.
(11) *Microbial Transformation and Degradation of Toxic Organic Chemicals*; Young, L. Y., Cerniglia, C. E., Eds.; Wiley-Liss Inc.: New York, 1995.
(12) Wyatt, J. M.; Knowles, K. C. *Int. Biodeterior. Biodegrad*. **1995**, *35*, 227−248.
(13) Huang, W.; Jia, J.; Cummings, J.; Nelson, M.; Schneider, G.; Lindqvist, Y. *Structure* **1997**, *5*, 691−699.
(14) Brennan, B. A.; Alms, G.; Nelson, M. J.; Durney, L. T.; Scarrow, R. C. *J. Am. Chem. Soc*. **1996**, *118*, 9194−9195.
(15) Miyanaga, A.; Fushinobu, S.; Ito, K. Wakagi, T. *Biochem. Biophys. Res. Commun*. **2001**, *288*, 1169−1174.
(16) Nagashima, S.; Nakasako, M.; Dohmae, N.; Tsujimura, M.; Takio, K.; Odaka, M.; Yohda, M.; Kamiya, N.; Endo, I. *Nature Struct. Biol.* **1998**, *5*, 347−350.
(17) Noguchi, T.; Honda, J.; Nagamune, T.; Sasabe, H.; Inoue, Y.; Endo, I. *FEBS Lett.* **1995**, *358*, 9−12.
(18) Tsujimura, M.; Odaka, M.; Nagashima, S.; Yohda, M.; Endo, I. *J. Biochem*. **1996**, *119*, 407−413.
(19) Noguchi, T.; Hoshino, M.; Tsujimura, M.; Odaka, M.; Inoue, Y.; Endo, I. *Biochemistry* **1996**, *35*, 16777−16781.
(20) Odaka, M.; Fujii, K.; Hoshino, M.; Noguchi, T.; Tsujimura, M.; Nagashima, S.; Yohda, M.; Nagamune, T.; Inoue, Y.; Endo, I. *J. Am. Chem. Soc*. **1997**, *119*, 3785−3791.
(21) Endo, I.; Nojiri, M.; Tsujimura, M.; Nakasako, M.; Nagashima, S.; Yohda, M.; Odaka, M. *J. Inorg. Biochem*. **2001**, *83*, 247−253.
(22) Murakami, T.; Nojiri, M.; Nakayama, H.; Odaka, M.; Yohda, M.; Dohmae, N.; Takio, K.; Nagamune, T.; Endo, I. *Protein Sci.* **2000**, *9*, 1024−1030.
(23) Noveron, J. C.; Olmstead, M. M.; Mascharak, P. K. *J. Am. Chem. Soc*. **1999**, *121*, 3553−3554.
(24) Tyler, L. A.; Noveron, J. C.; Olmstead, M. M.; Mascharak, P. K. *Inorg. Chem*. **1999**, *38*, 616−617.
(25) Tyler, L. A.; Noveron, J. C.; Olmstead, M. M.; Mascharak, P. K. *Inorg. Chem*. **2000**, *39*, 357−362.
(26) Mascharak, P. K. *Coord. Chem. Rev*. **2002**, *225*, 201−214.

conjunction with either carboxamido or imine nitrogens as donors undergo thiolate oxidation to form coordinated sulfi(e)nates and that the resultant Co(III) complexes are stable. However, no report on the effect of thiolate oxidation on the pK_a of water coordinated to such a Co(III) metal center has appeared. In order to determine the effect(s) of thiolate oxidation on the pK_a of bound water and related activity in model complexes such as **2**, we have recently directed our attempts toward isolation of the oxidized product(s). Herein, we report that addition of H_2O_2 to complex **2** affords K_2[Co(PyPSO_2(OSO_2)(CN)] (**3**), a species containing asymmetrically oxidized thiolates. The Co(III) metal center in **3** is coordinated to an S-bound sulfinate and an O-bound sulfonate (OSO_2) group and, unlike **2**, exhibits no loss of CN^- in aqueous solutions. It is therefore evident that oxidation of both thiolates leads to loss of lability at the Co(III) center in this type of model complexes. Addition of

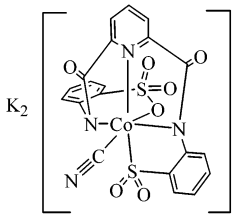

K_2[Co(PyP$\underline{S}O_2$($\underline{O}SO_2$)(CN)] (**3**)

H_2O_2 to **1** results in the isolation of $(Et_4N)_2$[Co_2(PyPS(SO_2))$_2$] (**4**), a dimeric species in which only the terminal thiolates are oxidized to form S-bound sulfinate groups while the bridging thiolates remain unchanged. Much like complex **1**, the Co−S−Co bridge in **4** can be cleaved with CN^- to afford $(Et_4N)_2$[Co(PyPS(SO_2))(CN)] (**5**), a species that contains both coordinated thiolate and S-bound sulfinate around Co(III). Complex **5** readily affords the corresponding aqua complex [Co(PyPS(SO_2))(H_2O)]$^-$ when dissolved in water, and the pK_a of the bound water in [Co(PyPS(SO_2))(H_2O)]$^-$ is 7.2 ± 0.06, one unit lower than the pK_a of the bound water in [Co(PyPS)(H_2O)]$^-$. These findings suggest that the oxidation of the Cys-S residues in Co−NHase modulates the pK_a of the bound water molecule. The synthesis and properties of complexes **1**−**5** and the pK_a measurements of the bound water in [Co(PyPS)(H_2O)]$^-$ and [Co(PyPS(SO_2))(H_2O)]$^-$ are described in detail in this paper. Preliminary hydrolysis studies indicate that [Co(PyPS(SO_2))(H_2O)]$^-$ promotes hydrolysis of acetonitrile at a lower pH (8.3) and at a faster rate compared to the hydrolysis of acetonitrile by [Co(PyPS)(H_2O)]$^-$ at pH 9.2.

Experimental Section

Materials. 2,6-Pyridinedicarbonyl dichloride, 2-aminothiophenol, sodium hydride, triethylamine, triphenylmethanol, triethylsilane, tetraethylammonium cyanide, potassium perchlorate, and trifluroacetic acid were procured from Aldrich Chemical Co. and used without further purification. Hydrogen peroxide (30%) was procured from Fisher Scientific Co. $[Co(NH_3)_5Cl]Cl_2$ was synthesized by following the published procedure.[31] All manipulations were carried out using standard Schlenk techniques except otherwise noted, and all solvents were dried and distilled before use.

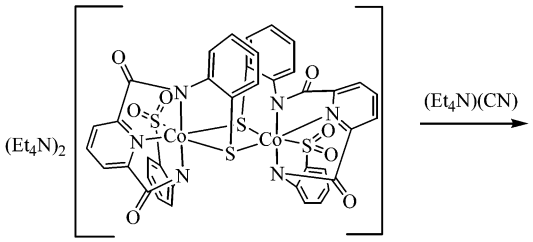

$(Et_4N)_2$[Co_2(PyPS($\underline{S}O_2$))$_2$] (**4**)

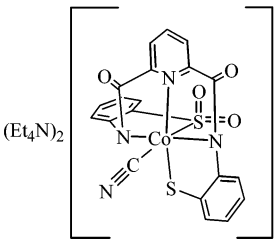

$(Et_4N)_2$[Co(PyPS($\underline{S}O_2$))(CN)] (**5**)

Synthesis. Safety Notes. *Caution!* Although no problems were encountered handling $KClO_4$ in this study, perchlorate salts are potentially explosive when heated.

Preparation of Compounds. PyPSH_4. The ligand, PyPSH_4, was synthesized by following the published procedure.[32]

$(Et_4N)_2$[Co_2(PyPS)$_2$] (1). A batch of 100 mg (4.2 mmol) of NaH was added to a solution of 402 mg (1.06 mmol) of PyPSH_4 in 20 mL of degassed dimethylformamide (DMF). The bright yellow solution was stirred for 10 min until all the NaH had reacted. Then, a batch of 266 mg (1.06 mmol) of $[Co(NH_3)_5Cl]Cl_2$ was added. The resultant slurry was heated to 70 °C for 1 h until a deep red-brown color developed. The solution was then cooled to room temperature, and 350 mg of $(Et_4N)Cl$ was added. After an additional 2 h of stirring, the DMF was removed under vacuum, and the brown residue was dissolved in 150 mL of acetonitrile (CH_3CN). The solution was filtered and the volume reduced to 40 mL. Next, 25 mL of diethyl ether (Et_2O) was added and the solution stored at −20 °C. After 12 h, $(Et_4N)_2$[Co_2(PyPS)$_2$] was collected as a dark brown microcrystalline solid. Yield: 720 mg (60%). Anal. Calcd for $(Et_4N)_2$[Co_2(PyPS)$_2$]·CH_3CN·0.3 H_2O (**1**·CH_3CN·0.3 H_2O, $C_{56}H_{65.60}N_9Co_2O_{4.30}S_4$ (1179.67)): C, 57.01; H, 5.60; N, 10.68. Found: C, 57.11; H, 5.49; N, 10.71. ^{1}H NMR (d_6-DMSO, 500 MHz, δ from TMS, 25 °C): 1.11 (Et_4N, t), 3.14 (Et_4N, q), 5.16 (1H, d), 6.27 (1H, t), 6.58 (1H, t), 6.76 (1H, d), 6.81 (1H, t), 6.90 (1H, t), 7.11 (1H, d), 7.64 (1H, d), 7.77 (1H, d), 8.09 (1H, t), 8.49 (1H, d). Selected IR bands: (KBr pellet, cm^{-1}) 1580 (ν_{CO}). Electronic absorption spectrum in CH_3CN, λ_{max}, nm (ϵ, per Co(III) metal center, M^{-1} cm^{-1}): 540 sh (4000), 430 (11 500), 310 sh (13 000).

$(Et_4N)_2$[Co(PyPS)(CN)] (2). A mixture of 200 mg (0.18 mmol) of **1** and 70 mg (0.44 mmol) of $(Et_4N)(CN)$ in 20 mL of CH_3CN was heated to reflux for 30 min. The reddish brown solution was then concentrated to 7 mL and cooled to −20 °C for 5 h. Crystalline

(27) Heinrich, L.; Li, Y.; Vaissermannn, J.; Chottard, J. C. *Eur. J. Inorg. Chem.* **2001**, 1407−1409.
(28) Heinrich, L.; Mary-Verla, A.; Li, Y.; Vaissermannn, J.; Chottard, J. C. *Eur. J. Inorg. Chem.* **2001**, 2203−2206.
(29) Rat, M.; de Sousa, A.; Vaissermann, J.; Leduc, P.; Mansuy, D.; Artaud, I. *J. Inorg. Biochem.* **2001**, *84*, 207−213.
(30) Kung, I.; Schweitzer, D.; Shearer, J.; Taylor, W. D.; Jackson, H. L.; Lovell, S.; Kovacs, J. A. *J. Am. Chem. Soc.* **2000**, *122*, 8299−8300.
(31) Schlessinger, G. C. *Inorg. Synth.* **1967**, *9*, 160−163.
(32) Noveron, J. C.; Olmstead, M. M.; Mascharak, P. K. *J. Am. Chem. Soc.* **2001**, *123*, 3247−3259.

Table 1. Summary of Crystal Data and Intensity Collection and Structure Refinement for $(Et_4N)_2[Co_2(PyPS)_2]\cdot CH_3CN\cdot 0.3H_2O$ (**1**·CH_3CN·$0.3H_2O$), $(Et_4N)_2[Co(PyPS)(CN)\cdot CH_3CN\cdot H_2O$ (**2**·CH_3CN·H_2O), $K_2[Co(PyPSO_2(OSO_2))(CN)]\cdot 3.5CH_3OH$ (**3**·$3.5CH_3OH$), and $(Et_4N)_2[Co_2(PyPS(SO_2))_2]\cdot 0.5CH_3CN\cdot CH_3OH\cdot 0.5H_2O$ (**4**·$0.5CH_3CN$·CH_3OH·$0.5H_2O$)

	$(Et_4N)_2[Co_2(PyPS)_2]\cdot CH_3CN\cdot 0.3H_2O$	$(Et_4N)_2[Co_2(PyPS(SO_2))_2]\cdot 0.5CH_3CN\cdot CH_3OH\cdot 0.5H_2O$	$(Et_4N)_2[Co(PyPS)(CN)]\cdot CH_3CN\cdot H_2O$	$K_2[Co(PyPSO_2(OSO_2))(CN)]\cdot 3.5CH_3OH$
formula	$C_{56}H_{65.60}Co_2N_9O_{4.3}S_4$	$C_{56}H_{68}Co_2N_{8.5}O_{9.5}S_4$	$C_{38}H_{56}CoN_7O_3S_2$	$C_{23.5}H_{25}CoK_2N_4O_{10.5}S_2$
mol wt	1179.67	1258.29	781.95	732.73
cryst color, habit	dark red prism	red needle	black parallelepiped	red plate
T, K	140(2)	90(2)	140(2)	92(2)
cryst syst	triclinic	monoclinc	monoclinic	triclinic
space group	$P\bar{1}$	$P2_1/n$	$P2_1$	$P\bar{1}$
a, Å	12.309(2)	10.001(2)	9.224(4)	10.2999(6)
b, Å	15.395(4)	25.003(4)	22.605(8)	15.7138(9)
c, Å	16.132(4)	22.571(4)	9.976(3)	20.0085(11)
α, deg	105.21(2)	90	90	69.111(2)
β, deg	102.43(2)	93.950(3)	106.00(3)	84.264(3)
γ, deg	102.51(2)	90	90	73.551(3)
V, A^3	2757.1(11)	5630.6(18)	1999.5(13)	2901.7(3)
Z	2	4	2	4
d_{calcd}, mg·m^{-3}	1.421	1.484	1.299	1.677
abs coeff, *μ*, mm^{-1}	0.809	0.803	0.58	1.086
GOF[a] on F^2	1.007	0.892	1.046	0.973
R1,[b] %	5.89	5.87	6.77	4.76
wR2,[c] %	11.05	12.68	13.57	11.20

[a] GOF = $[\Sigma[w(F_o^2 - F_c^2)^2]/(M - N)]^{1/2}$ (M = number of reflections, N = number of parameters refined). [b] $R1 = \Sigma||F_o| - |F_c||/\Sigma|F_o|$. [c] $wR2 = [\Sigma[w(F_o^2 - F_c^2)^2]/\Sigma[w(F_o^2)^2]]^{1/2}$.

2 was collected and dried under vacuum. Yield: 150 mg (57%). Anal. Calcd for $(Et_4N)_2[Co(PyPS)(CN)]\cdot CH_3CN\cdot H_2O$ (**2**·CH_3CN·H_2O, $C_{38}H_{56}N_7CoO_3S_2$ (781.95)): C, 58.36; H, 7.22; N, 12.54. Found: C, 58.21; H, 7.31; N, 12.35. ^{1}H NMR (d_6-DMSO, 500 MHz, δ from TMS, 25 °C): 1.12 (Et_4N, t), 3.07 (Et_4N, q), 6.50 (4H, m), 6.79 (1H, m), 6.84 (2H, d), 7.67 (2H, t), 7.99 (1H, t), 8.69 (1H, m). Selected IR bands: (KBr Pellet, cm^{-1}) 2111 (ν_{CN}), 1580(ν_{CO}). Electronic absorption spectrum in CH_3CN, λ_{max}, nm (ϵ, M^{-1} cm^{-1}): 560sh (1320), 460 (3000), 395 (3600).

$K_2[Co(PyPSO_2(OSO_2))(CN)]$ (3). A batch of 520 mg (0.72 mmol) of **2** was dissolved in 20 mL of CH_3CN, and 800 μL of 30% H_2O_2 was slowly added to it. Upon addition of the H_2O_2, an immediate color change from red-brown to orange was noted. After 1 h, the solvent was removed in vacuo, and the orange residue was dissolved in 2 mL of H_2O and loaded on an A-25-120 Sephadex column (Cl^- form, 5 cm × 30 cm). The column was eluted with a saturated aqueous solution of $KClO_4$, and the major orange band was collected. The water was carefully removed via rotary evaporation, and the excess $KClO_4$ was removed via extraction of the complex into CH_3OH and filtration. The bright orange solution thus obtained was concentrated to 10 mL. Slow diffusion of Et_2O into this solution resulted in orange microcrystalline **3**. Yield: 173 mg (42%). Anal. Calcd for $K_2[Co(PyPSO_2(OSO_2))(CN)]\cdot 3.5CH_3OH$ (**3**·$3.5CH_3OH$, $C_{23.50}H_{25}N_4CoK_2O_{10.50}S_2$ (732.73)): C, 38.52; H, 3.44; N, 7.65. Found: C, 38.41; H, 3.51; N, 7.59. ^{1}H NMR (d_6-DMSO, 500 MHz, δ from TMS, 25°C): 6.99 (1H, t), 7.14 (1H, t), 7.18 (2H, t), 7.33 (2H, t), 7.48 (1H, d), 8.00 (1H, d), 8.07 (1H, d), 8.38 (1H, t), 8.95 (1H, d). Selected IR bands: (KBr pellet, cm^{-1}) 2132 (ν_{CN}), 1618 (ν_{CO}), 1167, 1073, 1041 (all ν_{SO}). Electronic absorption spectrum in H_2O, λ_{max}, nm (ϵ, M^{-1} cm^{-1}): 520 (120), 395 sh (1600), 355 sh (2100).

$(Et_4N)_2[Co_2(PyPS(SO_2))_2]$ (4). A portion of 750 μL of 30% H_2O_2 was added dropwise to a solution of 300 mg (0.26 mmol) of **1** in 25 mL of methanol, and the mixture was stirred for 5 h at room temperature. The red-orange solution was then filtered, and the volume of the filtrate was reduced to 10 mL. Slow diffusion of Et_2O into this solution afforded long needles of **4** within 48 h. Yield: 160 mg (50%). Anal. Calcd for $(Et_4N)_2[Co_2(PyPS(SO_2))_2]\cdot$ MeOH·H_2O (**4**·MeOH·H_2O, $C_{55}H_{68}N_8Co_2O_{10}S_4$ (1247.26)): C, 52.96; H, 5.49; N, 8.98. Found: C, 53.03; H, 5.38; N, 8.91. ^{1}H NMR (d_6-DMSO, 500 MHz, δ from TMS, 25°C): 1.12 (Et_4N, t), 3.17 (Et_4N, q), 5.14 (1H, d), 6.30 (1H, t), 6.84 (1H, t), 6.98 (1H, t), 7.07 (1H, d), 7.39 (2H, m), 7.72 (1H, d), 7.80 (1H, d), 8.16 (1H, t), 8.40 (1H, d). Selected IR bands: (KBr pellet, cm^{-1}) 1616 (ν_{CO}), 1180, 1063, 1033 (all ν_{SO}). Electronic absorption spectrum (per Co(III) metal center) in CH_3CN, λ_{max}, nm (ϵ, M^{-1} cm^{-1}): 430 (6000), 360 sh (6600).

$(Et_4N)_2[Co(PyPS(SO_2))(CN)]$ (5). Complex **5** was synthesized by following a procedure analogous to the one used to synthesize **2**. A batch of 100 mg (0.08 mmol) of **4** was dissolved in 20 mL of CH_3CN, and a batch of 29 mg (0.18 mmol) of $(Et_4N)(CN)$ was added to it. The solution was then heated in a hot water bath at 65 °C for 30 min. Next, the solution was cooled to room temperature, and the CH_3CN was removed in vacuo. The purity of the burgundy microcrystalline product thus obtained was checked by ^{1}H NMR and used without further purification. Yield: 90%. Anal. Calcd for $(Et_4N)_2[Co(PyPS(SO_2))(CN)]\cdot CH_3CN$ (**5**·CH_3CN, $C_{38}H_{54}N_7CoO_4S_2$ (795.91)): C, 57.34; H, 6.84; N, 12.32. Found: C, 57.09; H, 6.90; N, 12.41. ^{1}H NMR (d_6-DMSO, 500 MHz, δ from TMS, 25°C): 1.16 (Et_4N, t), 3.18 (Et_4N, q), 6.15 (2H, m), 6.76 (1H, d), 6.86 (1H, t), 7.07 (1H, t), 7.16 (1H, d), 7.24 (1H, d), 7.68 (1H, d), 7.73 (1H, d), 8.05 (1H, t), 8.68 (1H, d). Selected IR bands: (KBr pellet, cm^{-1}) 2118 (ν_{CN}), 1580 (ν_{CO}) 1173, 1063, 1031 (ν_{SO}). Electronic absorption spectrum in CH_3CN, λ_{max}, nm (ϵ, M^{-1} cm^{-1}): 560 (1500), 440 (3050), 360 (5500).

X-ray Data Collection and Structure Solution and Refinement. Single crystals, suitable for X-ray diffraction, were obtained (a) by slow diffusion of Et_2O into a dilute solution of **1** in CH_3CN, (b) by slow diffusion of Et_2O into a dilute solution of **2** in CH_3CN, (c) by allowing a solution of **3** in CH_3OH to stand in an NMR tube for 30 days, and (d) by slow diffusion of Et_2O into a solution of **4** in 1:1 CH_3CN/CH_3OH. Diffraction data for complexes **1**−**4** were collected on a Bruker SMART 1000 diffractometer. All structures were solved by direct methods (SHELXS-97). The data were corrected for absorption effects.[33] Machine parameters, crystal data,

(33) Parkin, S.; Moezzi, B.; Hope, H. *J. Appl. Crystallogr*. **1995**, *28*, 53−56.

Table 2. Selected Bond Distances (Å) and Angles (deg)

bond distances				bond angles			
			$(Et_4N)_2[Co_2(PyPS)_2]\cdot CH_3CN\cdot 0.3H_2O$				
Co(1)−N(2)	1.853(4)	Co(1)−N(3)	1.925(4)	N(2)−Co(1)−N(3)	82.47(17)	N(3)−Co(1)−N(1)	163.47(16)
Co(1)−N(1)	1.945(4)	Co(1)−S(1)	2.2770(16)	N(2)−Co(1)−S(1)	102.91(13)	N(2)−Co(1)−S(2)	167.33(13)
Co(1)−S(2)	2.2210(16)	Co(1)−S(3)	2.3156(15)	N(1)−Co(1)−S(2)	107.58(12)	S(1)−Co(1)−S(3)	165.02(5)
Co(2)−N(5)	1.837(4)	Co(2)−N(4)	1.919(4)	S(2)−Co(1)−S(3)	84.07(6)	N(5)−Co(2)−N(4)	83.13(17)
Co(2)−N(6)	1.918(4)	Co(2)−S(4)	2.2865(15)	N(4)−Co(2)−N(6)	164.87(17)	N(5)−Co(2)−S(4)	98.84(13)
Co(2)−S(3)	2.2206(16)	Co(2)−S(2)	2.2922(15)	N(5)−Co(2)−S(3)	168.85(13)	S(3)−Co(2)−S(2)	84.63(6)
O(1)−C(7)	1.246(6)	O(3)−C(26)	1.234(6)	C(7)−N(1)−C(6)	118.2(4)	N(3)−C(13)−C(12)	109.8(4)
N(1)−C(7)	1.355(6)	N(4)−C(26)	1.365(6)				
			$(Et_4N)_2[Co(PyPS)(CN)]\cdot CH_3CN\cdot H_2O$				
Co(1)−C(20)	1.896(12)	Co(1)−N(2)	1.858(7)	C(20)−Co(1)−N(2)	87.2(4)	N(2)−Co(1)−N(3)	82.7(4)
Co(1)−N(1)	1.937(8)	Co(1)−N(3)	1.930(8)	C(20)−Co(1)−N(3)	95.6(4)	N(1)−Co(1)−N(3)	162.9(3)
Co(1)−S(2)	2.249(3)	Co(1)−S(1)	2.325(3)	N(2)−Co(1)−N(1)	81.8(3)	C(20)−Co(1)−S(2)	168.8(3)
O(2)−C(13)	1.255(13)	O(1)−C(13)	1.251(12)	C(20)−Co(1)−S(2)	86.4(3)	N(2)−Co(1)−S(1)	99.8(2)
N(1)−C(7)	1.350(12)	N(4)−C(20)	1.149(13)	N(2)−Co(1)−S(2)	168.4(3)	N(1)−C(7)−C(8)	111.2(9)
				N(1)−Co(S(2)	107.9(3)	N(4)−C(20)−Co(1)	175.2(10)
			$K_2[Co(PyPSO_2(OSO_2)(CN)]\cdot 3.5CH_3OH$				
Co(1)−C(20)	1.858(4)	Co(1)−N(2)	1.867(3)	C(20)−Co(1)−N(2)	87.14(14)	N(2)−Co(1)−N(3)	81.65(13)
Co(1)−N(1)	1.923(3)	Co(1)−N(3)	1.939(3)	C(20)−Co(1)−N(1)	91.33(15)	N(1)−Co(1)−N(3)	163.66(13)
Co(1)−O(5)	2.003(3)	Co(1)−S(1)	2.1883(10)	N(2)−Co(1)−N(1)	82.50(14)	C(20)−Co(1)−O(5)	176.17(13)
S(1)−O(2)	1.467(3)	S(1)−O(1)	1.472(3)	C(20)−Co(1)−N(3)	91.82(15)	N(2)−Co(1)−O(5)	96.69(12)
S(2)−O(7)	1.444(3)	S(2)−O(6)	1.455(3)	N(2)−Co(1)−S(1)	170.70(11)	O(2)−S(1)−O(1)	112.31(16)
S(2)−O(5)	1.491(3)	O(3)−C(7)	1.232(5)	O(7)−S(2)−O(6)	115.23(17)	O(7)−S(2)−O(5)	111.71(17)
O(4)−C(13)	1.238(5)	N(4)−C(20)	1.152(5)	O(6)−S(2)−O(5)	108.55(16)	N(1)−C(7)−C(8)	110.2(3)
				O(5)−S(2)−C(19)	107.72(17)	N(2)−C(12)−C(11)	119.6(4)
				N(4)−C(20)−Co(1)	175.9(3)	O(4)−C(13)−N(3)	127.7(4)
			$(Et_4N)_2[Co_2(PyPS(SO_2))_2]\cdot 0.5CH_3CN\cdot CH_3OH\cdot 0.5H_2O$				
Co(1)−N(2)	1.858(5)	Co(1)−N(3)	1.924(5)	N(2)−Co(1)−N(3)	82.9(2)	N(3)−Co(1)−N(1)	164.0(2)
Co(1)−N(1)	1.946(5)	Co(1)−S(1)	2.1977(17)	N(2)−Co(1)−S(1)	98.20(15)	N(2)−Co(1)−S(2)	168.20(15)
Co(1)−S(2)	2.2336(17)	Co(1)−S(3)	2.3301(17)	N(1)−Co(1)−S(2)	106.99(14)	S(1)−Co(1)−S(3)	166.18(7)
Co(2)−N(5)	1.845(5)	Co(2)−N(4)	1.923(5)	S(2)−Co(1)−S(3)	84.92(6)	N(5)−Co(2)−N(4)	82.6(2)
Co(2)−N(6)	1.942(5)	Co(2)−S(4)	2.1891(17)	N(4)−Co(2)−N(6)	163.4(2)	N(5)−Co(2)−S(4)	99.40(15)
Co(2)−S(3)	2.2292(17)	Co(2)−S(2)	2.3462(17)	N(5)−Co(2)−S(3)	168.35(17)	S(3)−Co(2)−S(2)	84.64(6)
S(1)−O(6)	1.473(4)	S(1)−O(5)	1.475(4)	O(6)−S(1)−O(5)	113.6(2)	O(8)−S(4)−O(7)	113.8(3)
S(4)−O(8)	1.465(4)	S(4)−O(7)	1.470(4)	C(7)−N(1)−C(6)	115.1(5)	N(3)−C(13)−C(12)	110.1(5)
O(1)−C(7)	1.236(7)	O(3)−C(26)	1.243(7)				
N(1)−C(7)	1.371(7)	N(4)−C(26)	1.344(7)				

and data collection parameters for complexes **1**−**4** are summarized in Table 1 while selected bond distances and angles are listed in Table 2.

Other Physical Measurements. Infrared spectra were obtained with a Perkin-Elmer 1600 FTIR spectrophotometer. Absorption spectra were measured on a Perkin-Elmer Lambda 9 spectrophotometer. ^{1}H NMR spectra were recorded on a Varian Unity Plus 500 running Solaris 2.6/VNMR 6.1B. The pK_a values of the bound water in $[Co(PyPS)(H_2O)]^-$ and $[Co(PyPS(SO_2))(H_2O)]^-$ were determined by fitting the plot of pH versus absorbance at 400 and 410 nm, respectively, with the aid of MATLAB package and by using the function $A = f_{HA}a_{HA} + f_{B^-}a_{B^-}$ where A is total absorbance, a_{HA} and a_{B^-} are the absorbances of the protonated and deprotonated species at the wavelength of measurement, and

$$f_{HA} = \frac{1}{\frac{K_a}{[H^+]} + 1} \qquad f_{B^-} = \frac{1}{\frac{[H^+]}{K_a} + 1}$$

Standard amide product analyses were performed on a Hewlett-Packard 5890 series II Plus gas chromatograph equipped with a flame-ionization detector (FID) and 10 m AT-Wax capillary column (Alltech). In a typical hydrolysis reaction, ∼30 mg of a model cobalt complex was dissolved in a mixture of CH_3CN and aqueous buffer (Tris-HCl) (total volume: 5 mL) in a screw-cap vial with a Teflon seal, and the mixture was kept in a constant-temperature bath. From time to time, aliquots of the reaction mixture were taken out and filtered through 0.25 μm Acrodisc nylon filter, and the filtrates were analyzed by gas chromatography. DMSO was used as the internal standard, and the products were identified and quantitated by comparison with authentic samples.

Results and Discussion

Although the deprotonated ligand $PyPS^{4-}$ afforded the monomeric Fe(III) complex $(Et_4N)[Fe(PyPS)]$,[32] the propensity of thiolato sulfurs to bridge[34−37] and the preference of low spin (d^6) Co(III) to adopt an octahedral coordination geometry in the presence of strong field ligands such as deprotonated carboxamido nitrogens[38,39] resulted in the formation of only the dimeric Co(III) complex $(Et_4N)_2[Co_2(PyPS)_2]$ (**1**) in the present work. Complex **1** is the precursor for all the complexes (**2**−**5**) reported in this account. The synthesis of **1** involves deprotonation of the ligand with NaH in DMF and $[Co(NH_3)_5Cl]Cl_2$ as the starting material. The initial heterogeneous reaction mixture is heated to allow

(34) Dance, I. G. *Polyhedron* **1986**, *5*, 1073−1104.
(35) Whitener, M. A.; Bashkin, J. K.; Hagen, K. S.; Girerd, J.-J.; Gamp, E.; Edelstein, N.; Holm, R. H. *J. Am. Chem. Soc*. **1986**, *108*, 5607−5620.
(36) Blower, P. J.; Dilworth, J. R. *Coord. Chem. Rev.* **1987**, *76*, 121−185.
(37) Hidai, M.; Kuwata, S.; Mizobe, Y. *Acc. Chem. Res*. **2000**, *33*, 46−52.
(38) Chavez, F. A.; Rowland, J. M.; Olmstead, M. M.; Mascharak, P. M. *J. Am. Chem. Soc*. **1998**, *120*, 9015−9027.
(39) Ray, M.; Ghosh, D.; Shirin, Z.; Mukherjee, R. *Inorg. Chem*. **1997**, *36*, 3568−3572.

complexation of the deprotonated ligands to the Co(III) metal center. When kept at room temperature, the reaction does not proceed even after 24 h. Despite the presence of thiolato sulfurs in the coordination sphere, **1** is resistant to oxidation by air. The Co−S−Co bridges in **1** are also resistant to cleavage when challenged with nucleophiles such as SCN^-, OH^-, pyridine, or *N*-methylimidizole. However, when CN^- is used as the nucleophile, the bridge is cleaved. Complex **2** is formed when **1** is heated with $(Et_4N)(CN)$ in CH_3CN for 30 min.

Although oxidation of bound thiolato sulfurs to S-bound sulfinato groups in Co(III) complexes has been achieved with excess H_2O_2,[24,25] addition of ∼20 equiv of H_2O_2 to **2** in CH_3CN results in a mixture of products including partial decomposition. Since **2** undergoes ligand exchange, oxidation of thiolate groups is not as clean as in substitutionally inert Co(III) "bis" complexes. Similar results have been reported by other groups.[27,29] Addition of 4 equiv of H_2O_2 to a solution of **2** in CH_3CN eventually affords complex **3**, which contains S-bound sulfinate and O-bound sulfonate (OSO_2) groups. The isomerization of S-bound sulfenate and sulfinate groups coordinated to Co(III) metal centers to the corresponding O-bound species has been well studied.[40−45] Additionally, Co(III) complexes with S- and O-bound sulfite (SO_3^{2-}) have been reported.[46−52] However, a search of the literature reveals only two other Co(III) complexes with coordinated sulfonate reported by Sargeson and co-workers.[53,54] One of these complexes comprises an O-bound $SO_3CF_3^-$ ligand while the other contains a coordinated sulfonate group (O-bound) that is part of a tridentate ligand frame. Neither complex is structurally characterized. Thus, complex **3** is the first structurally characterized Co(III) complex that contains both O-bound sulfonate and S-bound sulfinate groups. Formation of **3** suggests that as one of the thiolato sulfurs of **2** is overoxidized to sulfonate, the saturated sulfur center can no longer bind and S-to-O isomerization must occur. Oxidation of Ni(II) thiolates with H_2O_2 also affords O-bound sulfonate species.[55,56]

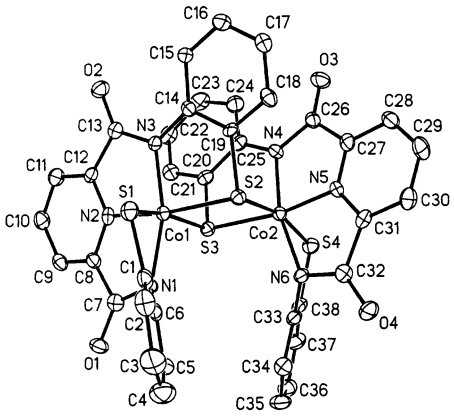

Figure 1. Thermal elliposoid (probability level 50%) plot of $[Co_2(PyPS)_2]^{2-}$ (anion of **1**) with the atom-labeling scheme. Hydrogen atoms are omitted for the sake of clarity.

The two types of thiolato sulfurs in **1**, terminal and bridging, exhibit different reactivity. For example, reaction of CH_3I with **1** results in the formation of $[Co_2(PyPS(SMe))_2]$[57] that contains terminal thioether groups but the bridging sulfurs remain unmodified. This lack of reactivity of the bridging thiolates is attributed to the lower basicity (low electron density) of such sulfur centers. Similarly, only the terminal thiolates in **1** react with H_2O_2 to form complex **4** in which the bridging sulfurs remain unoxidized. The robust nature of **1** allows one to use excess H_2O_2 without any complication. Since **4** contains asymmetrically oxidized thiolates, it offers the possibility of synthesizing a monomeric Co(III) species that contains both oxidized and unoxidized thiolato sulfurs such as the active site of Co−NHase. Indeed, when **4** is heated with 2.5 equiv of $(Et_4N)(CN)$ in CH_3CN for 30 min, complex **5** is formed in almost quantitative yield. The bridged structure of **4** is otherwise quite robust. Like **1**, reactions of **4** with other nucleophiles were unsuccessful. Complex **5** is very hygroscopic and can only be stored in a drybox. All attempts to isolate crystals of **5** for X-ray studies have so far been unsuccessful. However, analytical and spectroscopic data (vide infra) establish its structure beyond doubt.

Structure of $(Et_4N)_2[Co_2(PyPS)_2]\cdot CH_3CN\cdot 0.3H_2O$ ($1\cdot CH_3CN\cdot 0.3H_2O$). The dimeric structure of **1** is shown in Figure 1. Each Co(III) center is ligated to one pentadentate $PyPS^{4-}$ ligand with one thiolate from each ligand frame bridging to the other Co. The bridging thiolates complete the octahedral environment around the metal centers. The N_3S_3 coordination sphere thus formed around each metal center is composed of one pyridine nitrogen, two deprotonated carboxamido nitrogens, and three thiolato sulfurs. The three thiolato sulfurs are ligated in a *mer*-fashion with both ligand frames nearly planar except for a bend at N1 and N6. The bite angle of the 2,6-pyridinedicarboxamide unit gives rise to an average $N_{amido}-Co-N_{amido}$ angle of 164.17(16)°.

(40) Vitzthum, G.; Lindner, E. *Angew. Chem., Int. Ed. Engl.* **1971**, *10* (5), 315−326.
(41) Yamanari, K.; Shimura, Y. *Chem. Lett.* **1984**, 761−764.
(42) Mäcke, H.; Houlding, V.; Adamson, A. W. *J. Am. Chem. Soc.* **1980**, *102*, 6888−6889.
(43) Gainsford, G. J.; Jackson, W. G.; Sargeson, A. M. *J. Am. Chem. Soc.* **1982**, *104*, 137−141.
(44) Weber, W.; Maecke, H.; van Eldik, R. *Inorg. Chem.* **1986**, *25*, 3093−3095.
(45) Akhter, F. M. D.; Hirotsu, M.; Sugimoto, I.; Kojima, M.; Kashino, S.; Yoshikawa, Y. *Bull. Chem. Soc. Jpn.* **1996**, *69*, 643−653.
(46) Tewari, P. H.; Gaver, R. W.; Wilcox, H. K.; Wilmarth, W. K. *Inorg. Chem.* **1967**, *6*, 611−616
(47) van Eldik, R.; Harris, G. M. *Inorg. Chem.* **1980**, *19*, 880−886.
(48) Lange, B. A.; Libson, K.; Deutsch, E.; Elder, R. C. *Inorg. Chem.* **1976**, *15*, 2985−2988.
(49) Kapanadze, T. S.; Tsintsadze, G. V.; Kokunov, Y. V.; Buslaev, Y. A. *Polyhedron* **1990**, *9*, 1379−1382.
(50) Gibney, S. C.; Ferraudi, G.; Shang, M. *Inorg Chem.* **1999**, *38*, 2898−2905.
(51) Dash, A. C.; Patnaik, A. K.; Acharya, A. N. *Transition Met. Chem.* **1998**, *23*, 45−55.
(52) Kraft, J.; van Eldik, R. *Inorg. Chem.* **1985**, *24*, 3391−3395.
(53) Buckingham, D. A.; Cresswell, P. J.; Sargeson, A. M.; Jackson, W. G. *Inorg. Chem.* **1981**, *20*, 1647−1653.
(54) Jackson, W. G.; Sargeson, A. M. *Inorg. Chem.* **1988**, *27*, 1068−1073.
(55) Cocker, T. M.; Bachman, R. E. *Inorg. Chem.* **2001**, *40*, 1550−1556.
(56) Kaasjager, V. E.; Bouwman, E.; Gorter, S.; Reedijk, J.; Grapperhaus, C. A.; Reibenspies, J. H.; Smee, J. J.; Darensbourg, M. Y.; Derecskei-Kovacs, A.; Thompson, L. M. *Inorg. Chem.* **2002**, *41* (7), 1837−1844.
(57) Tyler, L. A.; Olmstead, M. M.; Mascharak, P. K. *Inorg. Chim. Acta* **2001**, *321*, 135−141.

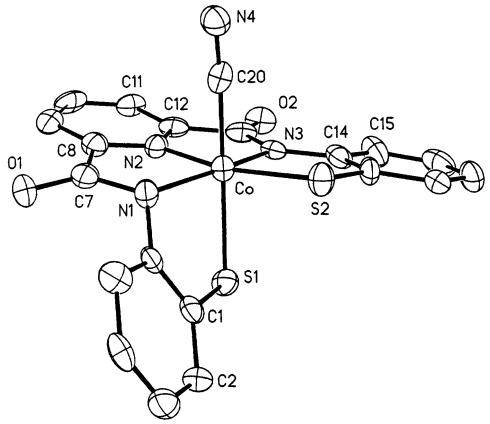

Figure 2. Thermal elliposoid (probability level 50%) plot of [Co(PyPS)(CN)]$^{2-}$ (anion of **2**) with the atom-labeling scheme. Hydrogen atoms are omitted for the sake of clarity.

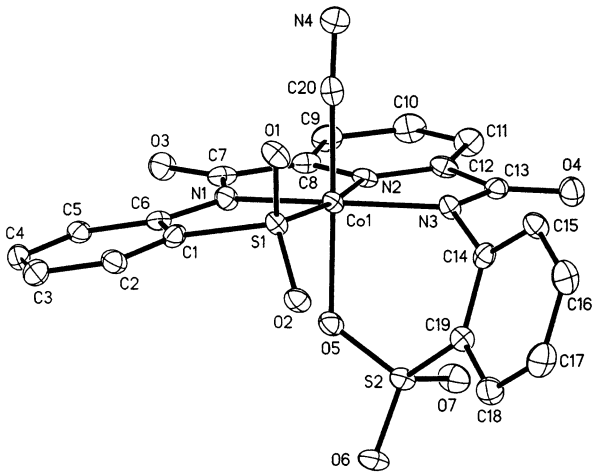

Figure 3. Thermal elliposoid (probability level 50%) plot of [Co(PyPSO$_2$(*O*SO$_2$)(CN)]$^{2-}$ (anion of **3**) with the atom-labeling scheme. Hydrogen atoms are omitted for the sake of clarity.

The average terminal Co−S_{thio} bond length (2.2818(16) Å) is within the range of those previously reported for Co(III) complexes with coordinated thiolates[25,58,59] and identical to the Co−S_{cys} bond distance reported for Co−NHase (2.28 Å).[15] The average Co−N_{py} and Co−N_{amido} bond lengths are 1.845(4) and 1.9268(4) Å, respectively, and are also within the range of those observed for similar complexes.[38,60,61]

Structure of $(Et_4N)_2$[Co(PyPS)(CN)]·CH_3CN·H_2O (2·CH_3CN·H_2O). Substitution of CN^- at the sixth site (in place of the bridging thiolate) on cobalt imparts little change to the coordination sphere; the mode of binding of the $PyPS^{4-}$ ligand to the Co(III) center in **2** and its octahedral geometry remain unchanged (Figure 2). The Co−C and the C≡N distances of the Co−CN unit (1.896(12) and 1.149(13) Å, respectively) lie in the range of such distances reported for other Co(III) complexes with ligated cyanide ions.[62,63] Interestingly, the Co−S_{thio} bond that is trans to CN^- is longer (by ∼0.08 Å) than the Co−S_{thio} bond that is cis to CN^-. The difference in bond length is attributed to the trans influence of the largely σ donating CN^- ligand. The S−Co−C bond angle is 168.8(3)° due to strains in the five-membered chelate rings.

Structure of K_2[Co(PyPSO_2(*O*SO_2))(CN)]·CH_3OH (3·3.5CH_3OH). Structurally, complexes **2** (Figure 2) and **3** (Figure 3) are similar. For example, the C≡N bond lengths in these complexes are nearly identical (1.149(13) and 1.152(5) Å, respectively). The Co−C bond length in **3** is, however, shorter than the analogous bond in **2**. This difference in Co−C bond length is attributed to the oxidation and subsequent isomerization of S-bound thiolate to O-bound sulfonate, a process that decreases the electron density at the metal center allowing the CN^- ligand to increase σ donation. Upon oxidation, the Co−S bond of **2** (av 2.267(3) Å) is shortened to 2.1883(10) Å in **3** (the Co−SO_2 bond length). Shortening of the Co−S_{thio} bond length upon oxidation of the sulfur center has been previously noted[64,65] and is attributed to increased ligand field strength. However, recent reports attribute this shortening of the M−SO_2 bond distance compared to the M−S distance to a decrease in the electrostatic interaction between the lone pairs on the thiolate (now used in bonding with the oxygens) and the metal d orbitals.[66]

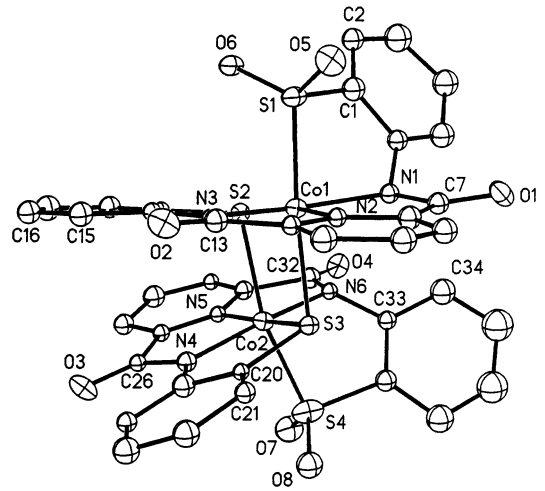

Figure 4. Thermal elliposoid (probability level 50%) plot of [Co_2(PyPS(*S*O_2))$_2$]$^{2-}$ (anion of **4**) with the atom-labeling scheme. Hydrogen atoms are omitted for the sake of clarity.

Structure of $(Et_4N)_2$[Co_2(PyPS(*S*O_2))$_2$]·0.5CH_3CN·CH_3OH·0.5H_2O (4·0.5CH_3CN·CH_3OH·0.5H_2O). The structure of complex **4**, shown in Figure 4, is very similar to that of **1** except for the fact that the terminal thiolates are oxidized to S-bound sulfinato groups (*S*O_2). Upon oxidation, a similar shortening of the Co−S_{thio} bond lengths is observed. The

(58) Freeman, H. C.; Moore, C. J.; Jackson, W. G.; Sargeson, A. M. *Inorg. Chem.* **1978**, *17*, 3513−3521.
(59) Elder, R. C.; Florian, L. R.; Lake, R. E.; Yacynych, A. M. *Inorg. Chem.* **1973**, *12*, 2690−2699.
(60) Angus, P. M.; Elliot, A. J.; Sargeson, A. M.; Willis, A. C. *J. Chem. Soc., Dalton Trans.* **1999**, 1131−1136.
(61) Chavez, F. A.; Olmstead, M. M.; Mascharak, P. M. *Inorg. Chem.* **1997**, *36*, 6323−6327.
(62) Dutta, S. K.; Beckmann, U.; Bill, E.; Weyhermüller, T.; Wieghardt, K. *Inorg. Chem.* **2000**, *39*, 3355−3364.
(63) Arzberger, S.; Soper, J.; Anderson, O. P.; la Cour, A.; Wicholas, M. *Inorg. Chem.* **1999**, *38*, 757−761.
(64) Adzamli, I. K.; Libson, K.; Lydon, J. D.; Elder, R. C.; Deutsch, E. *Inorg. Chem.* **1979**, *18*, 303−311.
(65) Lange, B. A.; Libson, K.; Deutsch, E.; Elder, R. C. *Inorg. Chem.* **1976**, *15*, 2985−2989.
(66) Grapperhaus, C. A.; Darensbourg, M. Y. *Acc. Chem. Res.* **1998**, *31*, 451−459.

Table 3. ν_{CN} Values in Complexes **2**, **3**, and **5**

complex	ν_{CN} (cm^{-1})
$(Et_4N)_2$[Co(PyPS)(CN)] (**2**)	2111
$(Et_4N)_2$[Co(PyPS(SO_2))(CN)] (**5**)	2118
K_2[Co(PyPSO_2(OSO_2))(CN)] (**3**)	2132
(Et_4N)(CN)	2075

Table 4. Comparison of Co−C and Co−Npy Bond Lengths

complex	Co−N_{py} (Å)	Co−C (Å)
$(Et_4N)_2$[Co(PyPS)(CN)] (**2**)	1.858(7) trans to RS^-	1.896 (12) trans to RS^-
K_2[Co(PyPSO_2(OSO_2))(CN)] (**3**)	1.868(2) trans to RSO^{2-}	1.858(3) trans to RSO_2O^-

mean Co−SO_2 bond length is 2.1934(17) Å, nearly 0.1 Å shorter than the average terminal Co−S_{thio} bond length. The Co−$S_{bridging}$ bond lengths are 2.2314(17) and 2.3382(17) Å while the mean Co−N_{py} and Co−N_{amido} bond distances are 1.852(5) and 1.934(5) Å, respectively. These bond lengths are similar to the reported bond lengths of **1** and other similar complexes.

Properties. Coordination of the deprotonated ligand $PyPS^{4-}$ to the Co(III) centers in **1** is confirmed by red shift of ν_{CO} from 1684 cm^{-1} in the free ligand to 1580 cm^{-1} in **1**. The shift in ν_{CO} to lower energy upon ligation of carboxamido nitrogen to metal center has been previously noted by our group and others.[67−69] The SO_x ($x = 2, 3$) groups in **3**−**5** give rise to strong bands in the range 1000−1200 cm^{-1} in the IR spectra of these complexes. Similar bands have been noted in previously reported Co(III) complexes with oxidized sulfur ligands.[40,64,70] Progressive oxidation of the thiolato sulfurs in **2** (forming **5** and **3**) results in a slight shift in the stretching frequency of the CN^- group (Table 3). The low values of this shift indicate that the C−CN bond is predominantly σ in character and there is very little change in the dπ−pπ* back-bonding as the sulfur centers are oxidized. The nearly identical C≡N bond lengths of **2** and **3** support this conclusion.

There has been some speculation regarding differences in the structural and kinetic trans effect of thiolato S centers versus SO_x ($x = 2, 3$) groups in metal complexes.[59,71] At least two groups report that the order of the structural trans effect in Co(III) complexes is $SO_3^{2-} \gg RSO^{2-} > S^-$ and that the kinetic trans effect follows the same trend. However, there is no information available on the trans effect of O-bound sulfonate group (RSO_2O^-). Structural data from this work (Table 4) suggest that the structural trans effects of RSO_2^- and RSO_2O^- are, respectively, greater and lesser than that of S^- in analogous Co(III) complexes. Unlike coordinated sulfite (SO_3^{2-}), O-bound sulfonate exerts much less of a structural trans effect. This is also in agreement with the kinetic trans effect. As described in a later section, **2** rapidly loses CN^- in aqueous solution while **3** does not.

The ^{1}H NMR spectra of complexes **1** and **4** contain 11 peaks for the 11 aromatic protons between 5 and 9 ppm (Figure S1, Supporting Information). A doublet at ∼5.2 ppm is typical for these dimeric complexes and has been assigned to the hydrogen atom(s) on C23 (and C35) that are situated between the two eclipsed aromatic rings in both structures (Figures 1 and 4). When the monomeric complexes are formed in reaction of **1** or **4** with (Et_4N)(CN), the peak at ∼5.2 ppm shifts downfield and all 11 protons resonate between 6 and 9 ppm in complexes **2**, **3**, and **5**. The shift of the ∼5.2 ppm peak in the ^{1}H NMR spectrum provides a convenient method of monitoring the bridge splitting reactions of **1** and **4** (Figure S2, Supporting Information). The conversion of **4** into **5**, as followed by ^{1}H NMR spectroscopy, is shown in Figure 5. The spectra indicate that reaction of CN^- and **4** affords **5** in a clean and quantitative manner. Likewise, ^{1}H NMR spectroscopy can also be used to follow the reverse reaction of monomers converting into dimers. Dissolution of **2** or **5** in D_2O results in the slow formation of **1** or **4**, respectively, following release of CN^-.

In the present work, we have employed $^{13}CN^-$ to synthesize ^{13}C-labeled **2**, **3**, and **5**. The ^{13}C NMR spectra of these complexes provide a convenient method of identification of the S-to-O isomerization process in this type of Co(III) complexes. In d_6-DMSO, ^{13}C-labeled **2** exhibits an enhanced peak at 133.83 ppm for the bound CN^- which shifts to 136.23 ppm in the case of ^{13}C-labeled **5**. It is therefore evident that oxidation of the thiolato sulfur trans to the bound CN^- results in a downfield shift of the CN^- resonance. However, when both thiolato sulfurs are oxidized to sulfinate and sulfonate, and the sulfonate moiety (trans to CN^-) is isomerized to afford **3**, the ^{13}C resonance for the bound CN^- shifts upfield to 113.52 ppm. Since free CN^- in d_6-DMSO resonates at 166.98 ppm, the ^{13}C NMR spectra of this type of complexes could be used for their identification. In addition, the chemical shift of the bound CN^- could provide clues toward the mode of binding of the SO_x group.

Much like the previously reported Co(III) complexes with coordinated thiolate,[24,25] the present complexes (except **3**) exhibit a thiolate-to-metal charge transfer (CT) band around 450 nm. This band along with absorption around 540 nm gives rise to the deep brown-red color of **1**, **2**, **4**, and **5**. Oxidation of the thiolato sulfurs in these complexes results in reduction of the intensity of these absorptions. Complex **3**, which contains O-bound sulfonate and S-bound sulfinate groups, exhibits a weak band at ∼520 nm[53,54] and no absorption at 450 nm. Collectively, it appears that this type of Co(III) centers exhibits absorption around 450 nm as long as one thiolato sulfur is coordinated to the metal center. Interestingly, Co−NHases exhibit strong absorption in 410−450 nm range.[72]

Reactivity. Dissolution of **2** in water (pH 7) results in rapid loss of CN^- and formation of the aqua species [Co(PyPS)-$(H_2O)]^-$ which has been identified by ^{1}H NMR spectroscopy. Although low spin d^6 Co(III) species are often described as

(67) Marlin, D. S.; Mascharak, P. K. *Chem. Soc. Rev.* **2000**, *29*, 69−74.
(68) Rowland, J. M.; Thornton, M. L.; Olmstead, M. M.; Mascharak, P. K. *Inorg. Chem.* **2001**, *40*, 1069−1073.
(69) Kawamoto, T.; Hammes, B. S.; Ostrander, R.; Rheingold, A. L.; Borovik, A. S. *Inorg. Chem.* **1998**, *37*, 3424−3427.
(70) Sloan, C. P.; Krueger, J. H. *Inorg. Chem.* **1975**, *14*, 1481−1485.
(71) Kastner, M. E.; Smith, D. A.; Kuzmission, A. G.; Cooper, J. N.; Tyree, T.; Yearick, M. *Inorg. Chim. Acta* **1989**, *158*, 185−199.
(72) Nagasawa, T.; Takeuchi, K.; Yamada, H. *Eur. J. Biochem.* **1991**, *196*, 581−589.

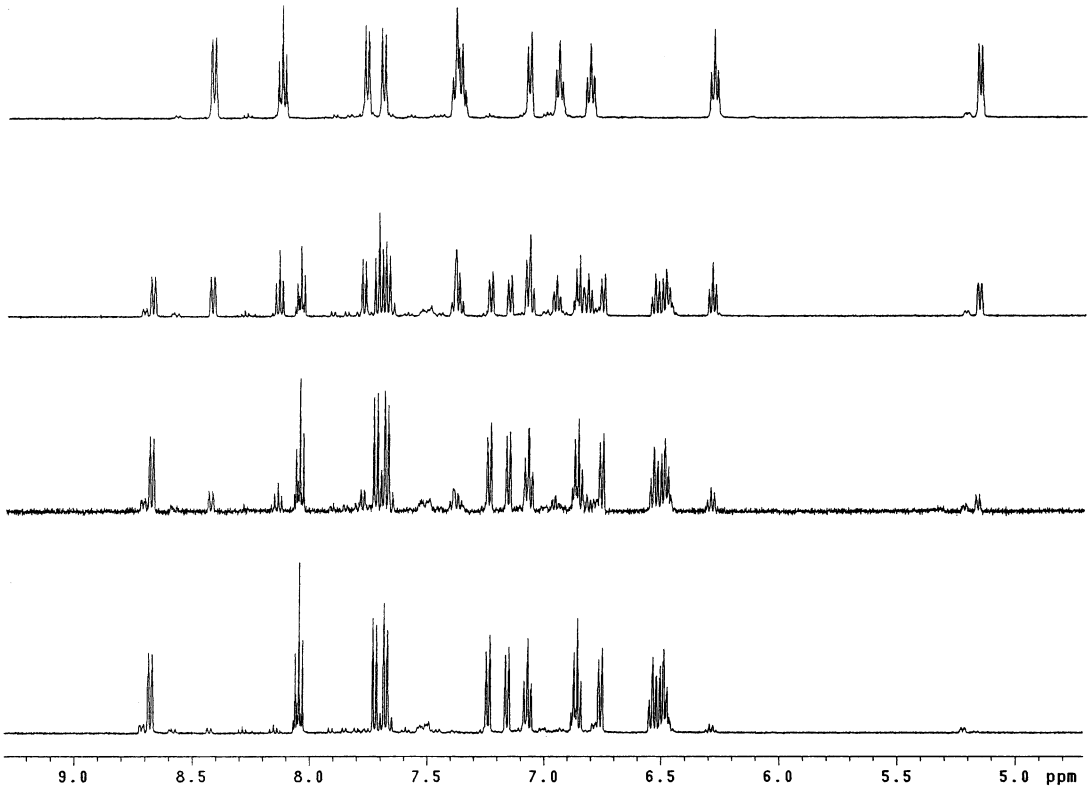

Figure 5. ^{1}H NMR spectra (500 MHz) showing conversion of **4** (top trace) into **5** (bottom trace) upon reaction with $(Et_4N)(CN)$ in CD_3CN (333 K). The spectra were run at intervals of 10 min.

kinetically inert,[73] examples of ligand exchange at Co(III) centers have been reported.[74,75] However, it is interesting to note that a Co(III) center with carboxamido nitrogen and thiolato sulfur donors (much like the Co(III) site in Co−NHase) exhibits fast ligand exchange in water. Since CN^- is a very strong ligand for Co(III), its rapid loss from **2** in water is particularly noteworthy. The facile substitution reaction at the Co(III) metal center of **2** has allowed us to determine the pK_a of H_2O bound in the sixth site of $[Co(PyPS)(H_2O)]^-$ by electronic absorption spectroscopy. When the pH of a solution of **2** in aqueous buffer is incrementally raised from 5 to 10, the peak at ∼420 nm splits into two bands at ∼390 and 440 nm indicating the formation of $[Co(PyPS)(OH)]^{2-}$ (Figure 6, Figure S3, Supporting Information). A plot of the pH values versus absorbance at 400 nm affords a value of 8.3 ± 0.03 for the pK_a of the bound water. This value is higher than the pK_a values of the bound water in Co(III) complexes of the type $[Co(L)(H_2O)]^+$ (L = N_5 ligands with two carboxamido nitrogens) which measure close to 7.[61,76] It thus appears that introduction of thiolato sulfur centers into the coordination sphere of Co(III) in addition to carboxamido nitrogens increases the pK_a of the bound water.

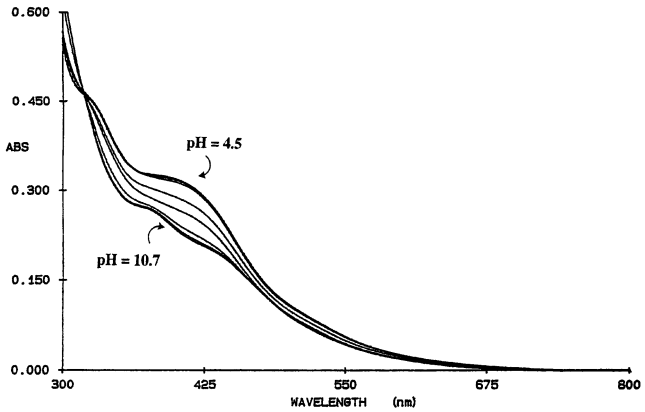

Figure 6. Changes in electronic spectrum of $(Et_4N)[Co(PyPS)(H_2O)]$ with pH in aqueous buffer. The spectrum at pH 10.7 is that of the $[Co(PyPS)(OH)]^{2-}$ species (for its ^{1}H NMR spectrum, see Figure S3, Supporting Information).

The optimal reactivity of Co−NHase is noted near neutral pH.[72] Since $[Co(PyPS)(H_2O)]^-$ exhibits a pK_a value of ∼8, it appears that the modified Cys-S centers could be responsible for enhancing the acidity (i.e., lowering the pK_a) of the bound water at the Co site in the enzyme. The availability of model complex **5** allowed us to test this hypothesis. When **5** is dissolved in water (pH 7), the orange color of the solution slowly turns yellow. The ^{13}C NMR spectrum confirms that **5** loses CN^- in aqueous solution, and the ^{1}H NMR spectrum indicates that a monomeric $[Co(PyPS(SO_2))(H_2O)]^-$ species is present in the aqueous solution. Unlike **2**, the ligand exchange reaction in the case of **5** is slow. For example, the

(73) Cotton, F. A.; Wilkinson, G. In *Advanced Inorganic Chemistry*, 5th ed.; Wiley: New York, 1988; pp 732−738.
(74) Kruse, W.; Taube, H. *J. Am. Chem. Soc*. **1961**, *83*, 1280−1284.
(75) Shearer, J.; Kung, I. Y.; Lovell, S.; Kaminsky, W.; Kovacs, J. A. *J. Am. Chem. Soc*. **2001**, *123*, 463−468.
(76) Chavez, F. A.; Nguyen, C. V.; Olmstead, M. M.; Mascharak, P. K. *Inorg. Chem*. **1996**, *35*, 6282−6291.

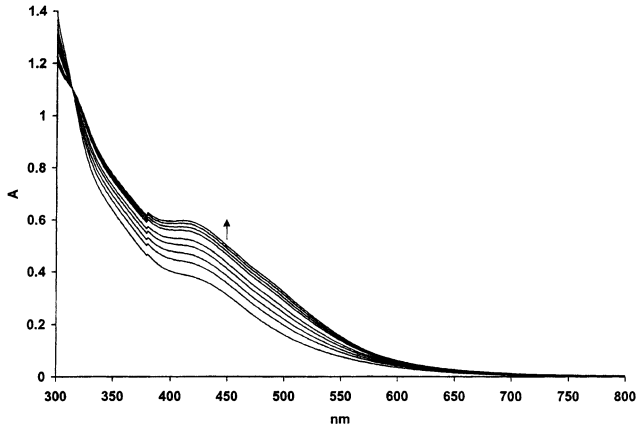

Figure 7. Changes in the electronic absorption spectrum upon conversion of $[Co(PyPS(SO_2))(CN)]^{2-}$ (bottom trace) into $[Co(PyPS(SO_2)(H_2O)]^-$ (top trace) in aqueous buffer at pH 6. The $t_{1/2}$ for this ligand displacement reaction is 40 min.

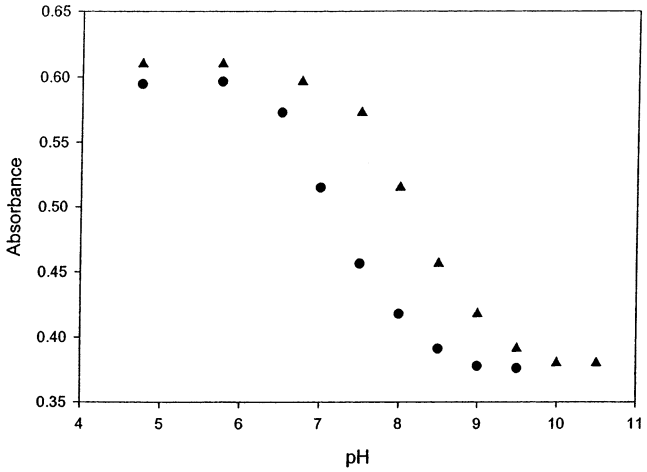

Figure 8. Plots of absorbances at 400 nm (for $[Co(PyPS)(H_2O)]^-$) and 410 nm (for $[Co(PyPS(SO_2)(H_2O)]^-$) vs pH. The pK_a values of the bound water in $[Co(PyPS)(H_2O)]^-$ and $[Co(PyPS(SO_2)(H_2O)]^-$ are 8.3 ± 0.03 and 7.2 ± 0.06, respectively.

$t_{1/2}$ of the ligand exchange (H_2O for CN^-) in the case of **5** is 40 min at pH 6 (Figure 7). This is quite in contrast to the almost instantaneous loss of CN^- in the case of **2**. The rate of exchange of CN^- with H_2O in the case of **5** also depends critically on pH. As the pH value is increased, the rate of exchange of CN^- by H_2O increases significantly. For example, the $t_{1/2}$ values for the exchange reaction at pH 6 and 9 are 40 and 3 min, respectively.

The pK_a of the bound water in $[Co(PyPS(SO_2))(H_2O)]^-$ has also been measured by electronic absorption spectroscopy. The plot of pH values versus absorbance at 410 nm affords a pK_a value of 7.2 ± 0.06 (Figure 8). This value is ~1 unit lower than the pK_a value of $[Co(PyPS)(H_2O)]^-$, the model complex without the oxidized sulfurs. The lower pK_a value of the bound water in the case of $[Co(PyPS(SO_2))(H_2O)]^-$ confirms that the oxidized sulfur center in **5** increases the acidity of the bound water. In turn, this result suggests that one of the roles of the modified Cys-S residues at the active site of Co−NHase is to modulate the acidity of the bound water.

In contrast to complexes **2** and **5**, complex **3** is inert and shows no sign of ligand exchange in aqueous solution. The CN^- is not lost from **3** even when reacted with $AgClO_4$. The material isolated in such reaction has been characterized by X-ray diffraction. The structure (Figure S4, Supporting Information) reveals that the addition of Ag^+ does not remove the CN^- ligand. Instead, a polymeric product is obtained in which the sulfonate (RSO_2O^-) group is no longer coordinated to the Co(III) center. A water molecule occupies the position vacated by the sulfonate group. The polymeric product comprises Ag^+ ions bridging Co(III) units via coordination to the sulfonate and carbonyl oxygens. Loss of lability at Co(III) centers in model complexes of Co−NHase has been noted in a few cases and has been attributed to greater Lewis acidity of the metal center following oxidation of the thiolato sulfur donors.[29] Since both the thiolato sulfurs are oxidized in **3**, it exhibits no exchange of CN^- in aqueous solution. Collectively, it appears that at least one thiolato sulfur is required in the coordination sphere of the Co(III) center of the model complexes to exhibit ligand exchange at the sixth site.

To date, a variety of roles have been suggested for oxidized Cys-S residues in proteins. For example, Cys-sulfenic (Cys-SOH) groups have been implicated in (i) reversible inhibition of tyrosine phosphatases and glutathione reductase, (ii) redox regulation of selected transcription factors, and (iii) peroxide reduction by NADH peroxidase.[77] In the case of Fe−NHases, the oxidized Cys-SOH and Cys-sulfinic (Cys-SO_2H) groups are believed to be involved in NO binding.[16] Although Co−NHases do not bind NO, work on co-substituted NHase of *Rhodococcus* sp. N771 indicates that both a low spin Co(III) center and the presence of one bound sulfinic group are essential for the NHase activity.[78] Studies on model complexes of Co-containing NHases also reveal key roles of sulfenato and sulfinato groups in the overall reactivity of the Co(III) center. For example, Artaud and co-workers have recently reported an increase in Lewis acidity of Co(III) centers in model complexes with a mixed N_{amido}/S_{thio} donor set[29] while Chottard and co-workers have suggested direct participation of the Co(III)-bound sulfenato groups in nitrile hydrolysis at acidic pH.[28] In the present work, we have demonstrated that the pK_a of the bound water in $[Co(PyPS)(H_2O)]^-$ is lowered by one unit upon oxidation of one of the thiolato sulfurs. Our results therefore indicate that the sulfinato group could increase the acidity of the bound water at biological Co(III) site.

Previously, we have reported that $[Co(PyPS)(H_2O)]^-$ (formed upon dissolution of **2** in water) promotes hydrolysis of CH_3CN at pH values above the pK_a of the bound water (~8.3).[23] Since no hydrolysis is noted at pH 7 and below, the involvement of a metal-bound hydroxide (in $[Co(PyPS)(OH)]^{2-}$) in the catalytic hydrolysis of nitrile is evident. Such a mechanism with metal-bound hydroxide as the key intermediate has been proposed by Nelson and co-workers.[13] In order to obtain further support in favor of this mechanism, we have now carried out hydrolysis of CH_3CN by **2** and **5**

(77) Claiborne, A.; Yeh, J. I.; Mallett, T. C.; Luba, J.; Crane III, E. J.; Charrier, V.; Parsonage, D. *Biochemistry* **1999**, *38*, 15407−15416.
(78) Nojiri, M.; Nakayama, H.; Odaka, M.; Yohda, M.; Takio, K.; Endo, I. *FEBS Lett.* **2000**, *465*, 173−177.

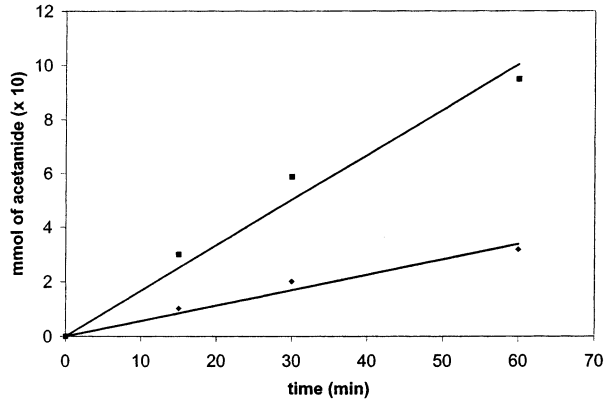

Figure 9. Hydrolysis of acetonitrile (to acetamide) by **5** (■) and **2** (◆) in pH 8 buffer at 40 °C. In each case, 0.04 mmol of the cobalt complex was dissolved in 3.5 mL of Tris buffer (pH 8) and 1.5 mL of acetonitrile in a screw-cap vial and kept at a constant-temperature bath. Samples were taken out every 15 min, and the amount of acetamide was checked by GC (see Experimental Section).

in aqueous buffer of pH 8. Since the pK_a values of the bound water in $[Co(PyPS)(H_2O)]^-$ and $[Co(PyPS(SO_2))(H_2O)]^-$ are ∼8.3 and ∼7.2, respectively, one expects a faster rate of hydrolysis in the case of $[Co(PyPS(SO_2))(H_2O)]^-$. Indeed, our preliminary experiment shows that **5** hydrolyzes CH_3-CN three times faster than **2** at pH 8 (Figure 9). The better catalytic performance of **5** at lower pH clearly indicates that (i) oxidation of the thiolato sulfur does increase the acidity of the bound water and (ii) a metal-bound hydroxide plays a key role in the hydrolysis of nitriles by model complexes that mimic the active site of the Co−NHase. Results of the hydrolysis of various nitriles by these model complexes under different conditions will be reported in a forthcoming account.

Acknowledgment. Financial support from an NIH grant (GM 61636) is gratefully acknowledged. L.A.T was a recipient of a GAANN fellowship from the U.S. Department of Education. We thank Todd Harrop and Dr. Robert Goldbeck for experimental assistance.

Supporting Information Available: ^{1}H NMR spectra of **1** and **4** (Figure S1), bridge-splitting reaction of **1** with CN^- followed by ^{1}H NMR spectroscopy (Figure S2), ^{1}H NMR spectrum of $[Co(PyPS)(OH)]^{2-}$ in D_2O (Figure S3), the structure of the polymeric product from the reaction of **3** with $AgClO_4$ (Figure S4), crystal structure data for **1**−**4** including atomic coordinates and isotropic thermal parameters, bond distances and angles, anisotropic thermal parameters, and H-atom coordinates (PDF). This material is available free of charge vis the Internet at http://pubs.acs.org.

IC030088S